Supporting information

Appendix S1. Distinct facets of geographical range shifts between historical and current periods.

Table S1 Description of the distinct facets of species' range shifts derived from the three outputs of the modeling framework: (1) historical species' range modeled using historical environmental and distribution records ("historical model"), (2) current species' range projected using the historical model and the current climatic conditions ("projected model"), and (3) current species' range modeled using current environmental and distribution records ("current model"). Outputs of the models are converted into presence-absence (i.e., 1-0) data.

	current climatic habitat	historical model	projected model	current model
persistence	*suitable*	1	1	1
persistence	*unsuitable*	1	0	1
colonization	*suitable*	0	1	1
colonization	*unsuitable*	0	0	1
extirpation	*suitable*	1	1	0
extirpation	*unsuitable*	1	0	0
lag	*suitable*	0	1	0

Appendix S2. Species' traits expected to affect range shifts.

Table S2 Description of species' traits and modalities.

Trait	Modality	Description
Body length	-	Total body length in adults (mm)
Larval length	1	< 4.2mm
	2	4.2-6.3mm
	3	> 6.3mm
Shape factor	-	Ratio of total body length to maximum body depth
Swimming factor	-	Ratio of the minimal depth of the caudal peduncle to maximum caudal fin depth
Fecundity	1	< 10000 oocytes
	2	10000-100000 oocytes
	3	> 100000 oocytes
Spawn time	1	1
	2	> 1
Egg diameter	1	< 1.35 mm
	2	1.35-2 mm
	3	> 2 mm
Life span	1	< 8 years
	2	8-15 years
	3	> 15 years
Female maturity	1	< 2 years
	2	2-3 years
	3	3-4 years
	4	4-5 years
	5	> 5 years
Parental care	1	No protection
	2	No protection with nest or egg hiders
	3	nest or egg hiders
Incubation period	1	< 7 days
	2	7-14 days
	3	> 14 days
Upper temperature limit	-	Upper limit of the optimal temperature range (°C)
Range size	-	% of total network length in the historical period
Elevational distribution preference	1	Low
	2	Medium
	3	High

From these traits, we defined species' ability to disperse by using one axis from a principal co-ordinates analysis (PCoA) based on four morphological traits: body sizes in adults and larvae, and ratios describing the hydrodynamic profile of the fish (shape factor) and their capacity for sustained swimming (swimming factor). For life-history strategies, we used the first axis (interpreted as life cycle duration) of a PCoA based on seven traits: female fecundity, spawn time, egg diameter, life span, female maturity, length of incubation period and parental care. Species' preferences along elevational gradient were defined following hierarchical clustering (Euclidean distance and Ward's linkage criterion) based on the range centre and the upper and lower range limits (Comte & Grenouillet, 2013).

Appendix S3. Model performances and changes in species' range between the historical and current periods.

Table S3 Predictive performances (cAUC) of the average models calibrated for each species, range changes (i.e., differences in spatial extent expressed as a percentage of the historical extent) and range similarities between current and historical periods. Numbers in brackets indicate standard deviations across the 30 modelling iterations. Three clusters (C1-C3) were defined following a hierarchical clustering based on the Ward's method with the Euclidean distance on the different descriptors of species' range shifts as defined in Fig. 1. The species status (N, native; NN, non-native) is indicated.

Species	Status	Historical cAUC	Current cAUC	Range change	Similarity	Cluster
Abramis brama	N	0.849 (0.021)	0.839 (0.021)	-1.3% (0.258)	0.322 (0.058)	C3
Alburnoides bipunctatus	N	0.866 (0.027)	0.867 (0.017)	-2.7% (0.203)	0.378 (0.034)	C3
Alburnus alburnus	N	0.891 (0.012)	0.894 (0.013)	+7.8% (0.183)	0.238 (0.040)	C3
Ameiurus melas	NN	0.865 (0.042)	0.847 (0.019)	+22.0% (0.357)	0.434 (0.068)	C1
Anguilla anguilla	N	0.891 (0.010)	0.909 (0.012)	+14.2% (0.162)	0.259 (0.044)	C1
Barbatula barbatula	N	0.808 (0.012)	0.799 (0.016)	+29.7% (0.270)	0.314 (0.087)	C1
Barbus barbus	N	0.894 (0.013)	0.892 (0.014)	-5.6% (0.126)	0.213 (0.031)	C3
Barbus meridionalis	N	0.929 (0.045)	0.923 (0.033)	+28.4% (0.458)	0.398 (0.078)	C1
Blicca bjoerkna	N	0.875 (0.030)	0.850 (0.024)	+36.6% (0.453)	0.401 (0.079)	C1
Chondrostoma nasus	N	0.871 (0.035)	0.905 (0.021)	-24.4% (0.181)	0.360 (0.075)	C3
Cottus gobio	N	0.828 (0.011)	0.849 (0.012)	+23.0% (0.272)	0.330 (0.054)	C3
Cyprinus carpio	NN	0.756 (0.033)	0.776 (0.026)	+26.6% (0.451)	0.498 (0.063)	C1
Esox lucius	N	0.829 (0.019)	0.840 (0.017)	-8.7% (0.126)	0.243 (0.035)	C3
Gasterosteus aculeatus	N	0.832 (0.023)	0.776 (0.031)	-10.9% (0.267)	0.425 (0.052)	C2
Gobio gobio	N	0.811 (0.012)	0.819 (0.018)	+4.1% (0.167)	0.244 (0.041)	C3
Gymnocephalus cernua	N	0.853 (0.044)	0.867 (0.021)	+24.4% (0.386)	0.426 (0.071)	C3
Lepomis gibbosus	NN	0.836 (0.027)	0.829 (0.015)	+4.3% (0.203)	0.388 (0.034)	C3
Leuciscus leuciscus	N	0.824 (0.017)	0.825 (0.013)	-8.5% (0.156)	0.261 (0.047)	C3
Lota lota	N	0.901 (0.035)	0.788 (0.079)	+34.8% (0.913)	0.615 (0.084)	C2
Parachondrostoma toxostoma	N	0.881 (0.056)	0.894 (0.028)	+11.8% (0.497)	0.417 (0.080)	C2
Perca fluviatilis	N	0.826 (0.016)	0.811 (0.015)	-6.7% (0.176)	0.261 (0.054)	C3
Phoxinus phoxinus	N	0.780 (0.014)	0.785 (0.017)	+15.8% (0.148)	0.401 (0.032)	C1
Pungitius pungitius	N	0.873 (0.025)	0.884 (0.018)	+33.9% (0.300)	0.368 (0.060)	C3
Rutilus rutilus	N	0.860 (0.012)	0.845 (0.015)	-9.2% (0.110)	0.209 (0.036)	C3
Salmo salar	N	0.910 (0.028)	0.893 (0.033)	+58.1% (0.536)	0.560 (0.052)	C1
Salmo trutta	N	0.870 (0.017)	0.866 (0.015)	-6.5% (0.050)	0.112 (0.022)	C3
Sander lucioperca	NN	0.864 (0.061)	0.835 (0.036)	+40.8% (0.613)	0.454 (0.089)	C1
Scardinius erythrophthalmus	N	0.773 (0.030)	0.786 (0.020)	+4.1% (0.334)	0.381 (0.068)	C3
Squalius cephalus	N	0.849 (0.011)	0.862 (0.020)	+4.3% (0.134)	0.214 (0.029)	C3
Telestes souffia	N	0.948 (0.026)	0.925 (0.020)	-1.1% (0.259)	0.381 (0.054)	C3
Thymallus thymallus	N	0.856 (0.047)	0.838 (0.048)	+23.5% (0.698)	0.684 (0.046)	C1
Tinca tinca	N	0.778 (0.020)	0.812 (0.019)	-28.2% (0.159)	0.427 (0.063)	C3

Appendix S4. Characteristics of the sampling sites between the historical and current periods.

Figure S1 Location of the sites sampled during the (a) historical and (d) current periods. Evolution of mean annual temperature and annual precipitation of sampled sites along the latitudinal gradient during the (b, c) historical and (e, f) current periods. Solid curves have been smoothed using a smoothing spline (d.f. = 3).

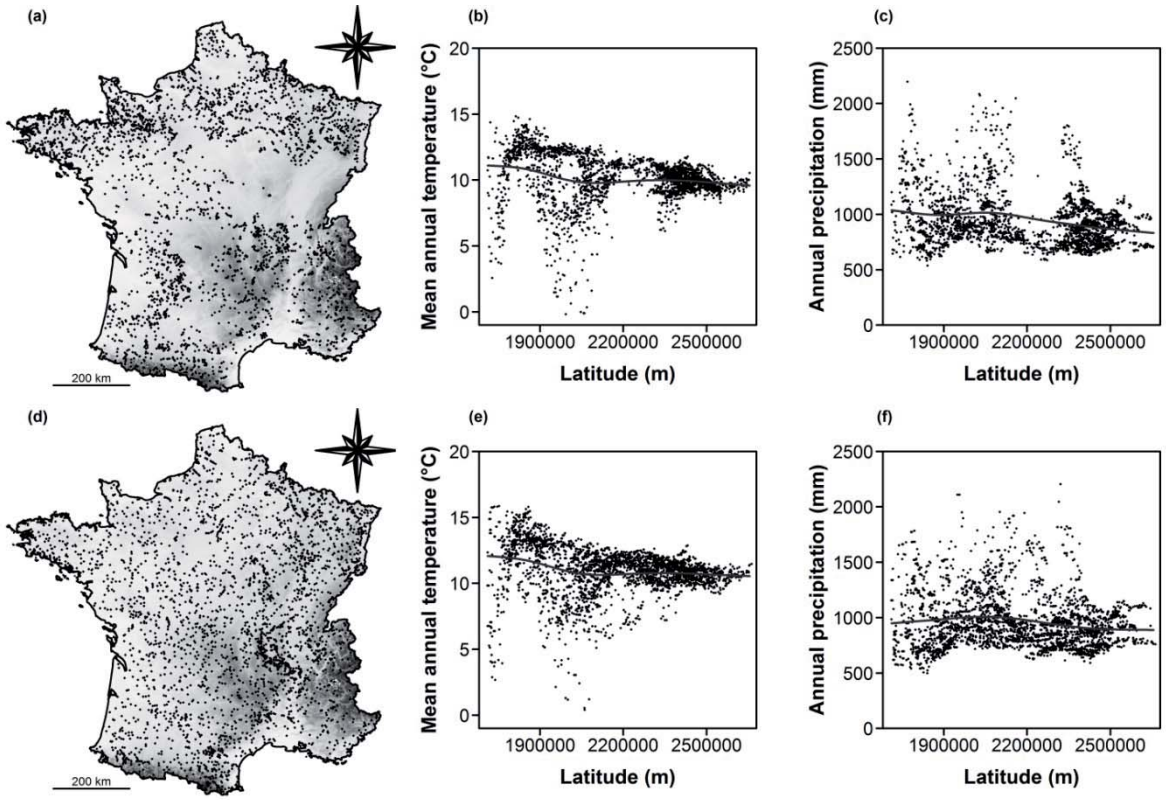

Appendix S4. Characteristics of the sampling sites between the historical and current periods.

Figure S2 Distribution of elevation, distance from source and slope of sampled sites during the (a, c, e) historical and (b, d, f) current periods.

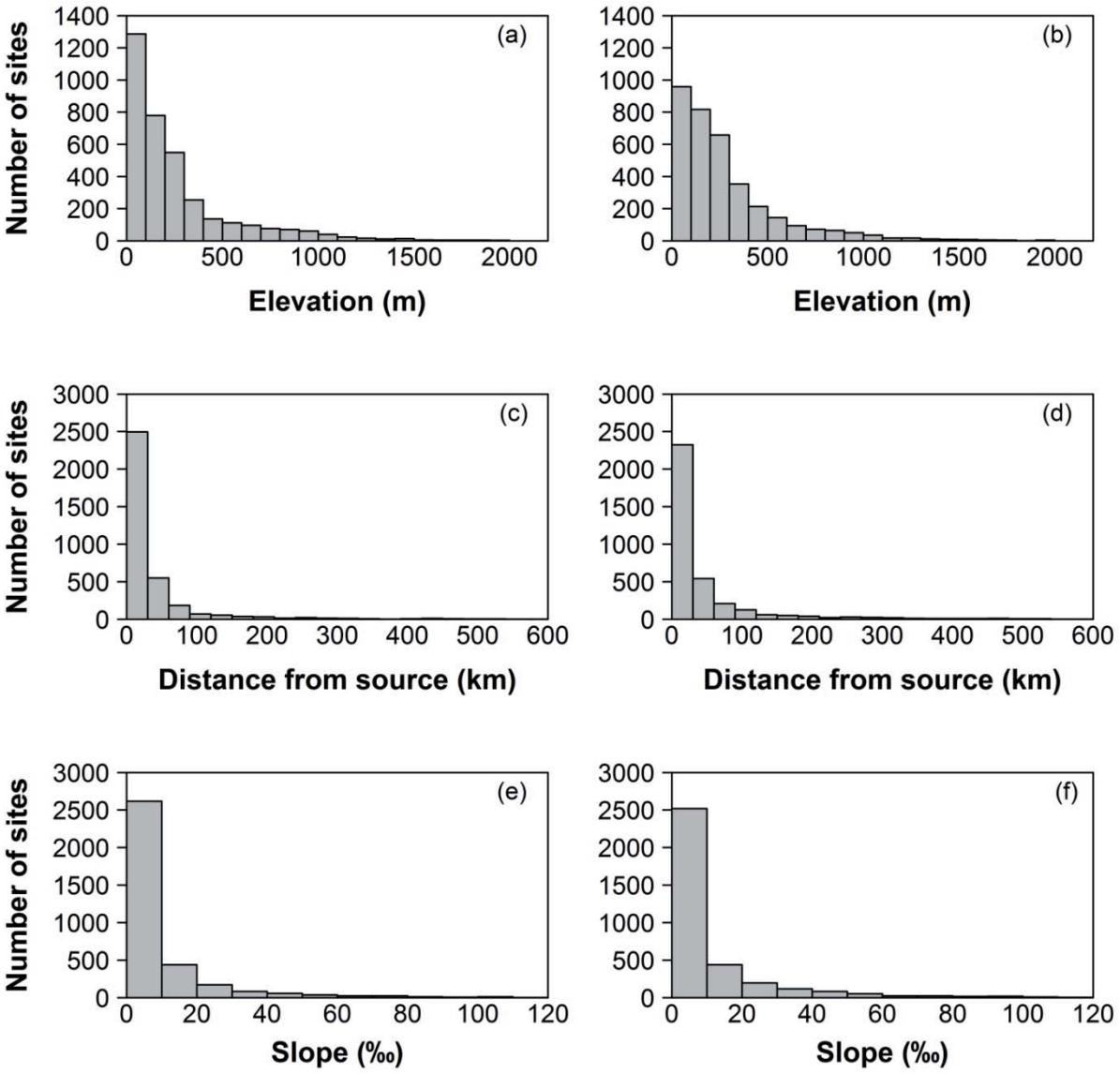

Appendix S4. Characteristics of the sampling sites between the historical and current periods.

Figure S3 Distribution of the timing of surveys during the (a) historical and (b) current periods. No significant difference was observed in mean survey date (expressed in Julian days) between the two periods (*t*-test, $P = 0.283$).